Characteristics of a Broadband Dye Laser Using Pyrromethene and Rhodamine Dyes

Sarah A. Tedder[1, 2,*], Jeffrey L. Wheeler[3], and Paul M. Danehy[1]

[1]*Advanced Sensing and Optical Measurement Branch, NASA Langley Research Center, 18 Langley Boulevard, Hampton, Virginia 23681-2199, USA*

[2]*Department of Physics, The College of William & Mary, P.O. Box 8795, Williamsburg, Virginia, 23187-8795, USA*

[3]*Whitworth University, 300 W. Hawthorne Road, Spokane, Washington, 99251-2515, USA*

[*]*Corresponding author: sarah.a.tedder@nasa.gov*

A broadband dye laser pumped by a frequency-doubled Nd:YAG laser with a full-width half-maximum (FWHM) from 592 to 610 nm was created for the use in a dual-pump broadband CARS system called WIDECARS. The desired broadband dye laser was generated with a mixture of Pyrromethene dyes as an oscillator gain medium and a spectral selective optic in the oscillator cavity. A mixture of Rhodamine dyes were used in the amplifier dye cell. To create this laser a study was performed to characterize the spectral behavior of broadband dye lasers created with Rhodamine dyes 590, 610, and 640, Pyrromethene dyes 597 and 650 as well as mixture of these dyes.

OCIS codes: 140.2050, 140.3538, 140.7300, 300.6230.

Introduction

Broadband dye lasers typically have bandwidth or full-width half-maximum (FWHM) determined only by organic dyes are used as a laser gain medium. The organic dye's complicated molecular structure generates a tightly-spaced energy spectrum which causes a "broadband" response to the excitation of the molecules [1], [2], [3]. Broadband dye lasers are used in a wide range of laser diagnostics applications such as degenerate four wave mixing (DFWM) [4], dye laser amplified absorption spectroscopy (intracavity absorption) [5], [6], broadband cavity enhanced absorption spectroscopy [7], and broadband CARS [4]. These broadband dye lasers have a variety of wavelengths and FWHMs each suitable for the intended application. Different types of dyes and solvents can be selected and mixed to tune the laser to the desired wavelengths for different applications.

A new variation of dual-pump broadband CARS, called Width Increased Dual-Pump Enhanced CARS (WIDECARS) [8], was designed to increase the number of species that can be measured simultaneously with CARS. This CARS system requires a broadband dye laser with a FWHM of 18 nm, from 592 to 610 nm, when pumped by a frequency-doubled Nd:YAG laser. Commonly, the organic dyes used to create a broadband dye laser near this desired spectral bandwidth range are Rhodamines because of their high efficiency and photostability [9]. The typical FWHM of a Rhodamine broadband dye laser is 4-10 nm [10-21]. A mixture of Pyrromethene dyes offer a FWHM of ~45 nm from 565-610 nm as demonstrated in Refs. [22] and [23]. These lasers are broader than what is desired for WIDECARS but include the wavelength range desired. Spectrally narrowing the emission will increase the energy per wavelength for the desired wavelengths. This narrowing can be accomplished by using spectrally selective optics similar to the methodology used to create narrowband dye lasers.

The spectral attributes of the WIDECARS broadband dye laser were not the only goals when designing this laser for a practical application of CARS. Because the broadband dye laser is only one component of the complicated setup that makes a CARS system, it is desirable for the laser to be easy to maintain and have simple construction. Another consideration was safety. Working in a hazardous environment increases the complexity of daily operation for CARS system operators and increases their risk of injury. Also, the energy output of the laser was desired to be similar to previously used broadband dye lasers. Finally, to reliably obtain accurate and precise measurements with the CARS system, the laser needs to have stable spectral characteristics throughout the testing day (8 hours) and as low as possible spectral noise (shot-to-shot variability).

The main body of this paper will include a detailed description of the experimental setup of the WIDECARS broadband dye laser and how its components affect the characteristics of its output. Specifically, the effects that dye concentrations, transmittance of a spectrally selective optic, and input energy (fluence) have on the efficiency, spectral bandwidth (FWHM), range, and wavelengths of the laser are described. Also included in this description is a study of the behavior of the spectral properties of broadband dye lasers produced by each of the Rhodamine and Pyrromethene dyes. The purpose of this study was to gain understanding of the behavior of broadband dye lasers created with each of these dyes and to allow others to use the behavior characterized to make a laser of their desired characteristics.

More detailed discussion is included about the WIDECARS laser. The effect of aging of the oscillator dye mixture used for the WIDECARS will be discussed for long exposures and long periods of no laser light exposure. Also included will be a description of the spectral noise of the WIDECARS laser to allow others to be able to decide if this laser has acceptable attributes

for their application. This paper will also describe in detail how the spectral shape of the broadband dye laser for WIDECARS was reached using these components and how it can be maintained.

Experimental Setup

A diagram of the optical setup of the broadband dye laser is shown in Fig. 1. The oscillator cell is side pumped (excited) by a frequency-doubled Nd:YAG laser (532 nm) pulsed for 10 ns at a 10 Hz repetition rate. The average maximum input energy to the oscillator cell is 37.9 ± 0.4 mJ. To maximize the conversion efficiency from the pump laser to the emitted laser, the pump laser is expanded in the horizontal direction to use the full length of the dye cell. This expansion is done with a 5.08 cm diameter concave cylindrical lens of -12 cm focal length, placed 21±.5 cm from the front face of oscillator cell. In the vertical direction the excitation light is focused with a 5.08 cm diameter, convex cylindrical lens of focal length 15 cm, placed 12±0.5 cm from the oscillator cell. The convex lens is mounted on a rotation mount so that the pump beam can be aligned with the path of the oscillator beam. The cross section of the pump beam on the front face of the oscillator cell is 22±1 mm by 4±1 mm.

The stable oscillator cavity is constructed with a 0.5 m radius convex back mirror and a 0.75 m radius concave output coupler, both with a diameter of 2.54 cm. The distance between these mirrors is 24.5±0.5 cm. The output coupler's coating is 50% reflective and is centered at 589 nm. The back mirror has a coating centered at 600 nm with a manufacturer reported reflectivity of greater than 99% for a 68 nm range. The oscillator dye cell is placed between the mirrors nearer to the output coupler, where the diameter of the oscillator beam is the largest allowing for a larger volume of the gain medium to be used. The dye cell dimensions are ~ 1.5 cm × 2 cm × 5 cm with its longest dimension perpendicular with the pump beam and parallel to

the oscillator beam. The dye cell's walls are at Brewster's angle with respect to the propagation direction of the oscillator beam. Gain media tested in this cell were a range of concentrations of Rhodamine 590, 610, and 640 in methanol and mixtures of these dyes. Also tested were a range of concentrations of Pyrromethene 597 and 650 in ethanol and mixture of these dyes. Ethanol was chosen as the solvent for the Pyrromethene dyes over methanol because they have higher solubility [24] and higher photostability in air-saturated ethanol than in air-saturated methanol [25].

A spectrally-selective optic can be placed within the oscillator, between the back mirror and the oscillator dye cell. Depending on the type of optic used, mirror or filter, this optic rejects or absorbs light of undesired wavelengths, respectively. The spectral region of light that this optic rejects or absorbs suppresses the gain of the laser in that region. This suppression allows increased gain in other spectral regions of the laser's frequency output operating on the same principle as tunable narrowband dye lasers. Just like narrowband dye lasers, the frequency selective optic channels all the stored energy into a narrower range of emission with low loss in power.

The rejection or absorption of light by an optic within an oscillator depends on its transmission spectrum. Transmission spectra of optics tested in the laser cavity are shown in Fig. 2. A thin film polarizer (TFP) from Rocky Mountain Instruments with part number TP2607K060, centered at 600 nm, has transmission curves as shown in by the thickest lines in red. This optic's transmission spectrum depends on the angle of incidence (labeled as θ in Fig. 1) and the polarization of the incoming light. The solid, dashed, and dotted curves, in Fig. 2, show the transmittance of the TFP for angle of incidences 60, 56, and 30 degrees, respectively. These curves were measured by the manufacturer. For each angle of incidence the transmittance is

different for parallel (P) and perpendicular (S) polarization directions over a range of wavelengths. P polarized light is transmitted at lower wavelengths than the S polarization, therefore separating the polarization of the light in this wavelength range. When placing this optic in the cavity the S-polarized light is rejected from the oscillator laser beam creating a P-polarized laser beam. Such an optic can act both as a polarizer and a frequency-selective optic.

Another optic tested is a yellow mirror centered at 550 nm; its transmission curves are shown in by the thinnest yellow lines in Fig. 2. These curves were measured with a spectraphotometer. The transmission of the yellow mirror also depends on the angle of incidence as shown by the difference between the solid, dashed, and dotted yellow curves. Optics with transmittances that have dependence on the angle of incidence allow for the control of the spectral shape of the laser output by changing of the angle of incidence. RG and OG filters transmission curves are shown in Fig. 2 by the medium thick lines in orange. These filters' transmittances are not dependant on their angles of incidence as they filter light by absorption rather than reflection.

The laser light from the oscillator cavity is passed through an amplifier cell located 25.4±0.5 cm away from the output coupler. The amplifier cell's dimensions are ~ 1 cm × 3 cm × 6 cm. It is oriented at Brewster's angle with respect to the propagation of the laser light. The laser is amplified in the cell with a mixture of Rhodamine dyes dissolved in methanol and pumped by light from the Nd:YAG laser. The beams are crossed in the cell at the smallest angle geometrically possible to maximize the overlap length in the cell and therefore increase the energy conversion efficiency. The maximum energy of the amplifier pump beam is 169 ± 1 mJ. To maximize the energy conversion, the cross sections of the beams are matched using a 2.54 cm diameter cylindrical lens with a 2 m focal length in the amplifier beam, placed 53.0±0.5 cm from

the amplifier cell. The cross sections of the beams are approximately 1 cm^2 as they enter the cell. So that the time overlap of the pump and broadband laser beam in the amplifier dye cell is optimum for energy conversion, the pump beam is delayed with a path 71.0±0.5 cm longer than the broadband.

The measurements used to characterize the broadband dye laser oscillator were taken between the output coupler and the amplifier dye cell. The amplifier measurements were taken after the amplifier dye cell and a collimating lens. Energies were collected with a pyroelectric detector power meter with a diffuser. The spectra were collected through a fiber optic cable to a spectrometer with a 0.48 nm resolution. Energy efficiencies were calculated using measured input and output energies in mJ. Spectral characteristics of the collected spectrum such as the FWHM (half maximum range), range (range of wavelengths at which the intensity is greater than 10% of the maximum intensity), and peak wavelengths were found using a code written specifically for this application. Figure 3 shows an example of a spectrum and the characteristics that the code determines. Some of the collected spectra were double peaked like the one in Fig. 3 and for these spectra two peak locations were measured. If between the two peaks the intensity of the spectra fell below the 50% of the maximum intensity, two half maximum ranges are collected – both based on the maximum peak, as shown in Fig 3. Similarly, two ranges were collected if the intensity fell below 10% of the maximum peak.

Results and Discussion

The wavelength, spectral shape, and efficiency of the laser are affected by every component of the laser. Components of the laser tested and characterized in this section are: dye type and concentration, the transmittance of the spectrally selective optics placed within the cavity, pump energy (fluence), and age of the dye solution. The output of the laser changes with

age whether the gain medium is pumped by laser excitation light or not. How each of these factors affects the FWHM (or half-maximum ranges), range (10% to 10% of maximum), efficiency, and wavelengths of the oscillator output will be presented. Next, the effects of amplifier dye type and concentration on the overall laser output will be presented and discussed. Finally, to allow users to more fully assess whether this laser design is usable for their application, the spectral noise of the laser will be reported. To illustrate how the results in this paper were used to design a laser with specific spectral characteristics, the broadband dye laser for WIDECARS is used as an example throughout all discussions.

In the pursuit of the desired spectral characteristics for WIDECARS, a variety of dyes and dye mixtures where tested to achieve the required 18 nm FWHM in the spectral range 590-610 nm. Mixtures of Rhodamine dyes were tested first, because they are desirable for their chemically safety and photostability [9]. The Rhodamine dyes with emission within the desired spectral range (590-610 nm) are Rhodamine 590, 610, and 640 (hereafter abbreviated R590, R610, and R640 respectively). Solutions of these dyes by themselves in methanol yielded a maximum FWHM of 7.2 nm. The two dye mixture of R610 and R640 achieved a maximum FWHM of 9.4 nm greater than the FWHM of any mixture of R590 with R610. This result was expected because the maximum reported FWHM in Refs. [15-20] using the mixture of R610 and R640 was 10 nm. These results are presented in further detail in Fig. 4 (a) in the next section. A mixture of all three dyes was attempted but the mixture's energy conversion efficiency decayed 35% after 4 hours of being mixed and 62% after 22 hours with limited laser excitation exposure, so the resulting emission characteristics are not reported here. This decay appears to be caused by some sort of interaction between R590 and R640, also reported by Ref. [26]. The other

Rhodamine dye combinations showed no such decay in this experiment or in others as reported in Refs. [16-21].

Because the desired spectral width for WIDECARS was not reached with the Rhodamine dyes, other dyes and setups were investigated. In Ref. [28] two separate dye cells were used with R590 and R610 to extend the tuning range of a narrowband dye laser and could possibly create a wider broadband dye laser. This setup was not used as it would add to complexity of the laser and would not meet the goal of a simple setup to maintain. A mixture of R590 and 4-dicyanomethylene-2-methyl-6-p-dimethylaminostyryl-4H-pyran (DCM) dyes might have been able to reach the desired broadband spectrum as the narrowband laser output in Ref. [27] shows a wide tuning range. But this mixture was not pursued because the hazardous nature of DCM would decrease the ease of use and safety of the laser. The other dyes available in the desired spectral range with high efficiency, good photostability [29] are Pyrromethene dyes. Unfortunately, these dyes aren't as photostable as the Rhodamine dyes but they have shown higher efficiencies [9]. Mostly importantly, Pyrromethene dyes have demonstrated a wide spectral response with a broadband dye laser [22] that includes the desired spectral range for WIDECARS. A range of concentrations of PM 597 and PM 650 in ethanol were tested along with a range of concentrations of mixture of these dyes.

Concentration

The dependence of the oscillator's spectral bandwidth (FWHM), range, wavelengths, and efficiency on concentrations of the Rhodamine and pure-Pyrromethene dyes can be seen in Fig. 4 (a-d). Figure 4 (a) shows the trend of the FWHM of R610 and R640 to increase slightly with concentration whereas the FWHM of the Pyrromethene dyes and R590 decrease with

concentration. This same trend is shown for R590 (Rhodamine 6G) in Ref. [30]. The bandwidth changes with concentration because of the re-absorption processes (described in the following paragraph) and quantum yield reduction (losses from nonradiative deexcitation [3]) [31] which increase with concentration. PM 650 has the largest FWHM for the range of tested concentrations and is the only dye, by itself, able to reach the needed size of the FWHM for WIDECARS, indicated by a green line in Fig. 4 (a). Off the scale in Fig. 4 (a), the largest FWHM of tested concentrations of PM 650 was ~54 nm at 52.55 mg/L is shown by black lines on either side of the squares in Fig. 4 (c). PM 597 dyes have the second largest FWHM in Fig. 4(a) and are broader that the Rhodamines. This was expected as the PM 597 shows a larger tuning range in narrowband laser operation in Ref. [24]. The range of the laser profiles versus the concentration shown in Fig. 4 (b) tells a similar story as the FWHM, except that the desired range can also be reached with low concentrations of PM 597.

The peak wavelengths versus oscillator dye concentrations are plotted with markers in Fig. 4(c), while the corresponding wavelength locations of the FWHM are plotted with solid lines. The peak wavelengths of the spectra shift to the red with increasing concentrations of R610, R640, PM 650, and PM 597. This is due to the singlet-singlet re-absorption (self absorption and re-emission) process as discussed in Ref. [32] and [33]. This process is a result of the frequency overlap of the absorption and emission bands of the dye. In the overlap the light that is emitted by the dye is self-absorbed and re-emitted to longer wavelengths. These longer wavelengths of light have a lower fluorescence emission cross-section (probability of emitting) which leads to a reduction in the FWHM and range of the laser profile, as noted in the previous paragraph. The desired 592 and 610 nm half maximum locations for WIDECARS are indicated in Fig. 4 (c) with green lines. PM 650 is the only dye shown that can reach the desired

width of 18 nm, but the wavelengths at which the spectrum is above its half maximum are not in the desired range of 592-610 nm. This leads to the conclusion that none of these dyes alone can reach the WIDECARS spectral profile goal.

In Fig. 4 (d), the oscillator efficiency of all the dyes increases until an optimum concentration is reached and then the efficiency levels off and eventually begins to decrease. This trend is caused by two competing effects. The concentration increases the efficiency of the laser by increasing the number of molecules available for stimulated emission. This trend continues until the number of molecules quenches the available excitation energy. Concurrently, the same re-absorption/re-emission effects that cause the red shift of the spectra with dye concentration [31], [34] also decrease the efficiency. As the concentration increases, more of the light is self-absorbed and re-emitted to longer wavelengths with lower and lower emission cross-sections, eventually causing the efficiency of the laser to decrease. The concentration for most efficient energy conversion in the oscillator depends on how well the excitation beam overlaps with the area of gain medium stimulated by reflected light from the mirrors. This dependence is shown by the two measurements of PM 597 in Fig. 4 (d). The triangles in Fig. 4 (d) were measured with low area overlap while the circles show the measurements of a higher area overlap of the light. The increased area of overlap increases the overall efficiency and decreases the concentration required for optimum energy conversion. All other dyes in Fig. 4(d) were taken with the lower area overlap of the pump and generated laser beams. The PM 597 is the most efficient of all the dyes and PM 650 is the least efficient. Pyrromethene dyes have higher efficiency than the Rhodamine dyes because of their lower probability of losing energy to mechanisms that don't produce stimulated emission. These reduced mechanisms of loss include lower intersystem crossing rates [29], reduced triplet-triplet absorption cross sections [35], and

lower aggregation formation, which all lead to a higher fluorescence quantum yield [36] (increased efficiency). PM 650 has efficiency that is atypical of Pyrromethene dyes because of an extra non-radiative deactivation process formed with an intramolecular charge transfer which is prominent in polar solvents such as ethanol [29]. Also PM 650 also has a relatively small Stokes shift (difference between peak absorption wavelength and the peak fluorescence wavelength) [37] which increases its self-absorption and therefore decreases its efficiency in comparison to other dyes.

Figure 5 shows the effect that adding relatively small amounts of PM 650 to higher concentrations of PM 597 has on spectrum of the oscillator. These relative concentrations (high PM 597 and low PM 650) were chosen to imitate the concentrations used in Ref. [22], where a spectrum with a FWHM from 565 nm to 610 nm was obtained. This range encompasses the desired wavelength range for WIDECARS (592-610 nm). While the spectra in Ref. [22] were too wide, it was hypothesized that similar but different ratios of dye concentrations could reach the desired WIDECARS spectrum. The spectral output of pure PM 597 is shown as a curve with square symbols in Fig. 5 with a peak near 580 nm. As very small amounts of PM 650 (in relation to the PM 597 concentration) is added to the mix, a second peak centered near 605 nm begins to emit and slowly increases in intensity and shifts to the red. Also, the peak from the PM 597 to shifts to the blue. In the mid PM 650 concentration range, a mixture is reached where the two peaks are high enough to create the large range as in Ref. [22]. As the PM 650 concentration increases further, the second peak becomes higher that the first and the entire spectrum shifts toward the red due to self-absorption. At the highest concentration of PM 650 the first peak from PM 597 has completely disappeared. This behavior of the dyes led to the discovery that, for this laser configuration, there exist no mixtures of Pyrromethene dyes that

can, by themselves, reach the desired FWHM in the wavelength range for WIDECARS, which is indicated in Fig. 5 as green thick curve. Therefore to achieve the WIDECARS spectral goal, further control of the spectrum, beyond dye concentration alone, is required.

The behavior of a PM 597 and PM 650 mixture can be explained by the acceptor-donor behavior of some dye mixtures. If fluorescence bands of a dye (PM 597) and the absorption band of another dye (PM 650) overlap, then energy can be transferred between the dyes. The fluorescence of the donor dye (PM 597) is absorbed by the acceptor dye (PM 650) which then fluoresces. This relationship is concentration dependant, as the absorbance by the acceptor dye increases with concentration, the emission from the donor decreases and the emission from the acceptor increases [38]. The acceptor-donor behavior of a PM 597 and PM 650 dye mixture was also reported in Ref. [39].

Figure 6 (a-d) shows the effect of the concentration of PM 650 on FWHM, range, peak locations, and efficiency on different concentrations of PM 597. As the concentration of PM 650 increases, the FWHM remains relatively constant until in the concentration range of 2-3 mg/L where the second peak raises above the half maximum.

This is the concentration range at which the acceptor dye (PM 650) is absorbing just enough energy from the donor dye to make the emission peaks from both dyes similar intensities. Similar peak heights occur at low concentrations of the acceptor because of the high efficiency of the energy transfer from the donor to the acceptor. In this concentration range of PM 650 dye, the maximum peak changes from the PM 597 emission to the PM 650 emission. This change in maximum emission is shown in Fig. 6 (a) by plotting the range of emission above the half maximum versus the concentration of PM 650. In Fig. 6 (a) the solid filled markers represent the half maximum ranges from the PM 597 emission and open markers represent the half maximum

ranges from the PM 650 emission. The maximum peak change is a result of the energy transfer of the donor to the acceptor which acts as a filter [40] reducing the emission from the donor. The concentration of PM 650 at which this transition occurs is relatively independent of the concentration of PM 597. This is because the fluorescence emission is independent of the donor concentration (PM 597) as demonstrated in Refs. [38] and [41]. The fluence at which the laser is pumped (in mJ/mm^2), determined by the pump beam energy and the size of generated beam and pump beam overlap, is also a factor that affects the donor-acceptor behavior of this dye mixture. Shown in blue diamonds, the FWHM for the higher area overlap (higher efficiency) increases the acceptor concentration required to create a large enough emission from PM 650 to exceed the half maximum. None of the dye mixtures tested in Fig. 6(a) reach the WIDECARS goal, indicated by a green horizontal line. The two emission profiles never merged to form the one large FWHM that was reported in Ref. [22], although the exact same dye mixture was tested. This may be due to the different fluence of the lasers, or perhaps different reflectivity of the laser cavity mirrors. Even if the two curves were to merge, the FWHM would exceed the WIDECARS goal, not meet it. In summary, the FWHM of a spectrum created from PM 597 and PM 650 is either less than the WIDECARS goal, has two separate half-maximum ranges, or has a much larger FWHM (using a laser configured as in Ref. [22]).

Figure 6 (b) shows the effect increasing PM 650 dye concentration has on the range. The range increases when the concentration of PM 650 is high enough to create a spectral profile that includes emission from both dyes, as seen in Fig. 5. Fig. 6 (b) shows that the concentration at which two emission peaks are present is relatively independent of the PM 597 as indicated from the behavior of the FWHM in Fig. 6 (a). However, the range is smaller for larger concentrations of PM 597. This is due to self-absorption of the PM 597, which shifts the laser emission from

this dye towards the red at higher concentrations, decreasing the distance between the emission peaks (seen in Fig. 6 (c)). In Fig. 6 (c) the locations of the peaks are shown for increasing concentrations of PM 650 at a range of PM 597 concentrations. If the spectrum has two peaks, two markers are shown at the same PM 650 dye concentration. Increasing the PM 650 concentration shifts the PM 597 emission peak to the blue as it is absorbed by the PM 650. The PM 650 peak emission shifts to the red as self-absorption increases with increasing PM 650 dye concentrations. Figure 6 (c) shows that the distance between the emission peaks decreases with increasing PM 597 dye concentration. This decrease occurs not only because of self-absorption of the PM 597 dye but also because the emission peak from the PM 650 dye is shifted toward the blue with increasing PM 597 dye concentration. This blue shift occurs because the energy available to transfer from PM 597 to PM 650 increases with increasing PM 597 dye concentration.

The effect of the pumping fluence (causing increase in efficiency of excitation) is seen in Fig. 6 (b) and (c). In Fig 6 (b), ranges shown with the blue outlined diamonds have similar concentration of PM 597 as the yellow diamonds but higher efficiency pumping (increased overlap of pumping area and generated laser beam). The better overlap pumping that causes the increase in range occurs at a higher concentration of PM 650. This same effect is seen in Fig. 6 (c) as the first occurrence of the second peak occurs at a higher concentration of PM 650, when the pumping fluence is higher.

Figure 6 (d) shows that the efficiency of the laser decreases with increasing concentration of PM 650. As the PM 650 concentration increases, the higher-efficiency PM 597 dye increases its donation of energy to the lower-efficiency PM 650. The rate of the decrease in efficiency depends on the concentration of PM 597 and on the pumping efficiency. The high-efficiency

pumping data show a smaller dependence on PM 597 dye concentration than the low efficiency pumping. The trends of the peak locations and efficiency (for high efficiency pumping) dependence on PM 650 led to the pursuit of a design of the laser that would have the lowest concentration of PM 650 as possible. This would give the laser the highest efficiency possible, while creating a spectrum with the desired location of the peak and half maximum for WIDECARS.

Spectrally Selective Optics

Spectrally-selective optics are commonly placed within laser cavities to produce a narrowed spectral output. These optics reject wavelengths depending on their transmission curves, suppressing gain for the wavelengths at which the optics have no transmittance. The transmitted wavelengths have preferential gain; therefore a laser with a desired spectrum can be created more efficiently than if the light is filtered outside the cavity. In the previous section it was discovered that although the desired spectrum for WIDECARS (592-610 nm) was unreachable using a combination of laser dyes alone, a larger range could be reached (565-610 nm). Therefore, it was reasoned that the desired spectrum could be created using a combination of dyes and a spectrally selective optic. After testing a variety of optics, the TFP centered at 600 nm was found to have a transmittance curve that could create the WIDECARS spectrum while also polarizing the laser output (as required for CARS). The TFP transmittance curve depends on the angle of incidence and therefore the spectral output of the laser can be tuned by changing in the angle of incidence. Figure 7 shows the spectral locations of the edges of the FWHM (location of half-maximums) for increasing concentrations of PM 650, for no optic and the TFP at a three different angles. All measurements for Fig. 7 where taken with the higher overlap of

pump and generated laser beam (higher efficiency pumping). Trend lines have been added to the figure for the reader to see the trend better but have no physical meaning. The shaded regions represent where the spectral intensity is greater than half of the maximum. The cavity with no optic (shown in triangles) has an almost constant FWHM that shifts to the blue as the PM 650 concentration increases. The blue shift occurs with increasing PM 650 dye concentration because more emission from the PM 597 is absorbed by the PM 650.

The angle of incidence of the TFP shifts the entire spectrum to the red as the angle increases. The location of the half-maximum on the blue side of the spectrum is mostly dependant on the TFP transmittance curve and changes ~2.6 nm/deg. This is because the blue side of the spectrum is emitted from the PM 597 dye and the location of its emission is almost independent of the PM 650 concentration, as seen in Fig. 6 (c). The red side of the FWHM shifts to the red with increasing PM 650. The red side of the FWHM also shifts to the red with decreasing angle of incidence, but the dependence decreases as the concentration of PM 650 increases. At the higher concentrations of PM 650, the gain that would have been transferred to higher wavelengths by selective optic suppression is transferred via the energy transfer from donor to acceptor dye. Using these relationships of the angle of the TFP and PM 650 dye concentration to the half-maximum locations, the blue side of the spectrum can be shaped with the selective optic and the concentration of PM 650 can be used to control the red side of the spectrum. In this way, a spectrum with any desired FWHM from 6-40 nm can be created, within the wavelength range from 570 nm-610 nm. The WIDECARS goals for the half-maximum locations are shown in Figure 7 by horizontal green lines and the goals are met with concentration of PM 597 of 49.08 mg/L and PM 650 of 4.6 mg/L and the TFP at an angle of 53 degrees.

Figure 8 (a) shows the dependence of the efficiency on the angle of incidence of the TFP for the same range of concentrations of PM 650 as shown in Fig. 7. The efficiency has the greatest dependence on the angle of incidence for pure PM 597 where the efficiency increases with the angle of incidence. As the concentration of PM 650 increases, the efficiency depends less on the angle of incidence of the TFP. The dependence on the angle decreases as wavelengths of the spectrum become more dependent on the donor-acceptor energy transfer than the transmittance suppression of the optic. At a concentration of 4.6 mg/L of PM 650 the efficiency is almost independent of the angle of incidence.

Figure 8 (b) is another representation of the data shown in Fig. 7, plotting the FWHM dependence on the angle of incidence of the TFP at difference concentrations of PM 650. Pure PM 597 shows the least dependence on the angle of incidence. As the concentration of PM 650 increases, the FWHM increases. Also, dependence of the FWHM on the angle of incidence of the TFP increases with higher concentrations of PM 650. In general, the FWHM increases with the angle of incidence. The higher concentrations show a leveling off or sudden decrease in the FWHM for higher angles of incidence. This change in trend occurs when the spectrum has two peaks and has intensity in-between these peaks that is below the half-maximum.

While the TFP centered at 600 nm was found to be the best optic for WIDECARS other optics may prove useful for other desired spectral profiles. A yellow mirror (transmission curve shown in Fig. 2) was also tested as the selective optic. The circles in Fig. 9 show the effect a range of yellow mirror angles have on a double-peaked dye mixture of 91.92 mg/L PM 597 and 10.58 mg/L of PM 650 (not the same as the WIDECARS mixture). For easier viewing, the measured values in Fig. 9 are fitted with trend lines: the thin lines represent the range, the thickest lines are the FWHM, and dashed lines are the peak wavelength. The lines with no

markers show the spectral profile of the dye mixture with no optic in the cavity. Interestingly, at an angle of incidence of 40 degrees the yellow mirror suppresses the emitted spectrum in such a way that the space between the two peaks is filled, creating a much wider spectrum. The triangles in Fig 9 show the effect of the TFP on this same dye mixture; note its narrower spectra. The effect created by the yellow mirror hasn't been as fully investigated as the TFP. Fig. 9 demonstrates that there is a wide range of spectra that could be created using different types of selective optics and mixtures of PM 597 and PM 650. Schott RG and OG filters were also tested in the laser cavity, resulting in other spectral profiles. These filters weren't tested extensively because their transmission spectra do not vary with angle of incidence and therefore cannot be used to fine-tune the shape of the laser spectral profile.

Fluence

Fluence of the laser is the energy density of the pump on the gain medium. Figure 10 (a) and (b) shows how the fluence of the laser affects the efficiency and spectral output of the laser. Increasing fluence increases the efficiency of the laser whether the gain medium is pure PM 597 (triangles) or a mixture with PM 650 (the WIDECARS mixture is shown in circles in Fig. 10). The fluence in Fig. 10 is controlled by changing the power of the laser; where as in Fig. 4 above the fluence was controlled by a change in the overlap of the pump and generated laser beams. The fluence used to pump the laser has a minimal effect on the spectral profile of pure PM 597, as seen in Fig. 10 (b) (triangles) and in Fig. 4 (a, b, and c) for concentrations ~50 mg/L. But when PM597 is in a mixture with PM 650 its properties change as it becomes a donor for PM 650. The effect of fluence on the spectral profile of a donor-acceptor mixture of PM 597 and PM 650 is shown in circles in Fig. 10 (b). The donor-acceptor energy transfer is highly efficient

therefore the acceptor dye emission quenched at a low fluence. As the fluence increases, the remaining excitation energy, not transferred to the acceptor dye, increasingly stimulates emission of the donor dye. The effect of this is shown in Fig. 10 (b) by a shift of the blue side of the spectrum further to the blue as the donor dye emission begins to increase. As the donor dye increases it spectral output the acceptor dye emission is consistent; therefore the FWHM and range of the spectrum increases. This is the same as the effect seen in Fig. 6 (a-c) in the concentrations needed to create emission peaks from the acceptor dye (PM 650). For example, in Fig. 6 (b), the lower efficiency pumping required a smaller concentration of PM 650 to increase the range because more of the donor's emission was absorbed by the acceptor.

Amplifier

Rhodamine dyes were chosen as the gain medium for the amplifier because of their good photostability [25]. Using dyes with good photostability reduces the need for regular maintenance. Because this laser was designed to be used in an already high-maintenance CARS system, easy maintenance was included in the design goals. The spectral profile of the light from the oscillator can be changed when passed through the amplifier. This is demonstrated in Fig. 11 (a) and (b) which compare the wavelengths of the peaks, half maximums, and ranges for spectra emitted from the oscillator to spectra emitted from the amplifier. The oscillator dye mixture for the data presented in Fig. 11 is ~89 mg/L PM 597 and ~1 mg/L PM650 and was pumped in the low efficiency configuration. Fig. 11 (a) compares spectra emitted from the oscillator with constant concentration (open circles) to the amplifier (filled circles) for increasing concentrations of R640 in methanol as the gain medium. When pure R640 dye was used in the amplifier, the oscillator spectrum was narrowed. The amplified spectrum shifted to the red with increasing

R640 dye concentration. To reach the desired WIDECARS spectra an amplifier gain medium was sought that would cause minimal narrowing. Mixtures of R610 and R640 were found to cause less narrowing, and some results are shown in Fig. 11 (b). As a secondary consideration, the concentrations were also optimized for power amplification. Using the dye mixture 49.08 mg/L PM 597 and 4.6 mg/L PM 650 with high efficiency pumping in the oscillator the WIDECARS spectral profile was obtained with the amplifier concentrations of 21.7 mg/L R610 and 8.4 mg/L R640. Compared to the oscillator output, this mix creates a ~1 nm shift to the red with no narrowing. These concentrations increased the oscillator energy output by ~2 times. Typical overall efficiencies of the laser with the WIDECARS spectral profiles are 7-8%. These efficiencies were calculated by finding the ratio of the overall output energy to the sum of the pumping energy of the oscillator and the amplifier. Optimum concentrations for other possible spectral profiles were not investigated.

Aging

The emission of lasers change with time (age), because of photodegradation when exposed to light and because of chemical reactions in the dark. Photodegradation is a reaction between a molecule and light that causes the molecule to breakdown (change in structure). As the organic dye gain medium photodegrades, the concentration of absorbing and emitting dye molecules decreases, changing the emission spectra just as a change in concentration would. Pyrromethene dyes photodegrade faster than Rhodamine dyes [25], [42]. Pyrromethene dyes' predominant pathway of photodegradation is a reaction with singlet oxygen [35]. When excited to the triplet state, Pyrromethene dyes transfer energy to ground state oxygen (if present) and

produce singlet oxygen [1]. The dyes reaction with singlet oxygen leads to the breakdown of the dye molecular structure.

PM 650 dye tested in Ref. [29] and [44] showed a higher photostability than PM 597. But Ref. [29] and [45] showed that in solvents with high electron-donor capacity, PM 650 decayed with age even in the dark. Ethanol, the solvent used for this experiment, is not a high capacity electron-donor, but there was a noticeable decay of the PM 650 dye emission with age even with only limited light exposure. The decay observed may be a photodegradation as the solution was not stored in complete darkness.

In the mixture of the PM 650 and PM 597 dyes, the PM 650 photodegradation rate is faster than PM 597, as observed by Ref. [39]. This faster rate is most likely caused by an excited state electron energy transfer, as discussed for similar Pyrromethene dyes in Ref. [46]. The electron energy transfer is from the excited state of the acceptor dye to the ground state of the donor dye. The faster decay of the Pyrromethene acceptor dye may be the cause of the observed decay of the PM 650 dye. This process could occur when exposed to ambient light not just excitation light.

The change of photophysical attributes (laser emission spectra) was measured by collecting the emission spectra of a solution of PM 597 and PM 650 over time for multiple angles of the TFP. Using spectral attributes of the emission, such as locations of the half maximums and range, the rate of their change in nm/day was collected. The measured decay rates in nm/day were compared to the effect of varying the concentration of PM 650 on the emission spectra (nm/(mg/L)) to obtain the rate of loss of emission from the PM 650 dye in (mg/L)/day. The rate of loss of efficiency from photodegradation, was not used for these measurements of PM 650 decay. This is because the laser emission contains excited light from

both dyes: the measured efficiency is affected by both dyes. The efficiency of the laser increases as the PM 650 decays but the efficiency from the PM 597 decreases with exposure.

The decay rate was measured under two conditions: one when the dye was measured over a long period of time, 17 days, with minimal exposure to light and a second, where the dye was exposed to excitation light continuously for a full testing day (~8 hours). The first condition measured a loss of 0.19 (mg/L)/day of PM 650 concentration emission. The second condition measured 1.13 (mg/L)/day decay of PM 650. Each of these measurements includes the influence of the other. While the dye is exposed to excitation light the mechanism causing decay without exposure to light excitation will still occur. And the decay rate of dye without light exposure could not be measured without exposing the dye to laser light. To minimize this effect the dye was exposed to laser excitation light for as short as possible time periods when measuring the non-laser light excitation decay rate.

These measured decay rates allow laser operators to estimate the amount of PM 650 to add to the solution to obtain a desired spectral output after the dye has decayed. For example, if the dye mixture had the desired spectra output 2 days ago and was excited by laser light for a total of 5 hours then to obtain the same spectral attributes 0.615 mg/L (2 days×0.19 (mg/L)/day + 5 hours×0.047 (mg/L)/hour) of PM 650 should be added.

The decay of PM 650 dye in the oscillator is also studied by measuring the change of the lasers spectral profile after it passes through the amplifier. These amplified spectral profiles are used to create CARS. Therefore the rates of change of these profiles represent the rates of change experienced by the CARS spectra during an experiment. The rate of change of the spectra from the amplifier in terms of decay of the PM 650 dye in the oscillator are slower than from the oscillator. When minimally exposed to laser excitation light decay rate of the spectrum

was 0.16 (mg/L)/day. The decay rate measured during exposure to excitation light continuously was 0.52 (mg/L)/day decay of PM 650.

One of the goals of the WIDECARS laser was to have a spectral profile that was constant for a typical testing day of 8 hours. To have accurate measurements with CARS, the spectral profile of the broadband dye laser must be accurately characterized and divided from the measured spectra. If changes of the broadband dye laser profile over time are large, then the normalization will be lead to inaccurate CARS temperature and concentration measurements. To assess if the variation of the spectral profile of the WIDECARS broadband dye laser is acceptable, the new laser's non-resonant CARS spectra aging rates have been compared to a non-resonant CARS spectra aging rates using the all-Rhodamine broadband dye laser from Ref. [47]. Because any changes in the spectra are important, including shifts in the spectra, the rate of decay was calculated using the shape of the non-resonant spectra. The change in the shape of the spectra over time was calculated by finding the average percentage difference of intensity per pixel between normalized spectra taken at different times during a testing day. The rate of change in shape for both types of lasers Rhodamine and WIDECARS were ~1% change per hour.

Although the rate of change of the WIDECARS is similar to the Rhodamine dye laser which may be acceptable for some experiments, the more consistent the laser profile over time the better the accuracy of the CARS measurement. The stability of the laser profile could be improved by decreasing the photodegradation of the laser. Because the photodegradation of the PM 650 dye is caused by singlet oxygen, it is possible to decrease the rate of decay by adding singlet oxygen quenchers such as DABCO [35] and [42]. No such additive was added to the laser described in the present work to avoid decreasing the safety of the laser as DABCO is a

chemical hazard. Another possible solution to decrease the decay rate is to deoxygenate the dye mixture [25] and [42]. This is less effective than chemical additive but still increases the half-life of the dyes [42]. While deoxygenating is hard to implement without any leaks in the large volume and complicated circulation system [42], it would offer a less hazardous alternative. It was mentioned earlier that lower Pyrromethene dye concentrations were chosen for the WIDECARS laser because they lead to higher efficiency. Lower concentrations of Pyrromethene dyes are also beneficial for photodegratation as the dyes will photodegrade slower at lower concentrations as shown in Ref. [48].

Spectral Noise

The spectral noise (shot-to-shot variations) of a broadband dye laser's spectral profile can affect the uncertainty of the measurement system in which it is applied. For CARS the temperature and species concentration measurements uncertainties scale mainly with the spectral noise in the broadband dye laser's profile [49]. Change in the overall intensity of the laser is not an issue when the CARS spectra are normalized during the data analysis as they are for WIDECARS. The measured CARS spectrum includes shape of the broadband dye laser. This shape is removed by first measuring gas that has no resonant species in the CARS wavelength excitation range. The measured CARS spectrum is then divided by this measured shape of the broadband dye laser. This shape is an averaged spectrum and typically is not measured for each laser pulse (camera shot). Therefore changes in the shape of the laser shot-to-shot are not accounted for. This causes errors in the normalization leading to shot-to-shot inaccuracy and increased uncertainty in the measurements.

To assess the spectral noise (shot-to-shot variability) of this new laser, the standard deviation in percent was calculated at each wavelength and is plotted in Fig. 12. The spectrometer used to collect spectra used in the calculations for Fig. 12 is unable to resolve the narrow mode structures of the dye laser. Therefore the modes in each spectrum collected are averaged across many modes and the noise measured is decreased from the actual noise. All measurements in Fig. 12 were made with the same resolution and therefore offer accurate relative measurements of the spectral noise.

In Fig. 12 both the oscillator and amplifier averaged output and percentage standard deviations are plotted. The amplifier has smaller deviations than the oscillator output. To compare the standard deviations to a dye laser like the one used in Ref. [47], a Rhodamine 610 broadband dye laser averaged output and relative standard deviation is shown. Comparing the standard deviations of the amplified WIDECARS laser and the Rhodamine 610 laser at the peak of their spectra, the WIDECARS laser is more stable. The WIDECARS standard deviations minimum is just below 2%, where the Rhodamine dyes lasers minimum standard deviations is just above 2%. Towards the outside of the WIDECARS laser (590-595 nm and 605-610 nm) the standard deviations are similar to the majority of the Rhodamine dye laser range (3-4%). Outside these ranges the variation continues to gradually increase. These trends suggest that it is best to use the peak of the spectrum and that WIDECARS laser will not introduce more uncertainties than traditionally used Rhodamine dye lasers. The wavelength range of reduced standard deviation for the WIDECARS is larger than for the narrower Rhodamine dye laser. An unconventional “modeless” dye laser has shown to improve precision of temperature measurements in single-pump CARS systems. These lasers have reduced standard deviations in the peak of the dye laser profile down to ~1% as reported in Ref. [19].

Conclusion

In conclusion, a laser with the desired attributes for a WIDECARS system was developed. A range of dyes for the gain medium were tested. The gain medium that produced the desired results was a mixture of 49.08 mg/L PM 597 and 4.6 mg/L PM 650 for the oscillator and 21.7 mg/L R610 and 8.4 mg/L R640 for the amplifier. While this mixture of PM 597 and PM 650 creates a laser output over the desired spectral range, the profile created using these dyes does not have a FWHM of the desired width. Spectrally selective optics were placed in the oscillator cavity to test if their transmission could shape the broadband dye spectra to the desired laser profile. A TFP centered at 600 nm and placed at an angle of incidence of 53 degrees was found to provide the desired spectral shape, width and center wavelength. As a secondary consideration to the desired laser spectral profile, oscillator and amplifier dye mixtures were chosen to have maximum efficiency, though the resulting efficiency was lower than many other dye lasers.

Other goals of the WIDECARS laser were achieved such as simple construction, safety, and ease of maintenance. The laser has almost the same construction as a typical broadband dye laser, only adding a selective optic in the cavity. The dye lasers offers no more safety hazard than a typical broadband dye laser made with only Rhodamine dyes because Pyrromethene dyes have similar safety guidelines. The PM 650 dye showed a noticeable photodegradation rate over a testing day creating a change in the spectral profile during the day. The rate of this change is similar to a broadband dye Rhodamine dye laser. The PM 650 photodegradation rate has been quantified so the laser spectral profile can be easy to maintain. A possible solution to make the photodegradation rate slower is to deoxygenate the solution; this was not tested and could be pursued further. The other components of the laser are identical to previously-used broadband

dye lasers and therefore will have similar maintenance requirements. The spectral noise was slightly lower in comparison to Rhodamine broadband dye lasers predicting a similar instrument uncertainty capability for CARS measurements.

While pursuing the WIDECARS laser spectral profile, many other spectral profiles were created and documented in this paper. The results presented provide readers who have different spectral requirements, guidelines for reaching their goals within the capabilities of this general laser design. Many other spectrally selective optics or dye combinations or fluences possible with this laser setup were not tested but could be investigated in the future. For example, PM 597 and PM 650 were not tested as the amplifier gain mixture. While for WIDECARS this may not be desirable, as it could lead to an increase in maintenance as these dyes photodegrade faster, this may produce a new range of spectral profiles.

Acknowledgements

The authors would like to thank Stephen Jones for his support in the laboratory. This work was funded by NASA's Fundamental Aeronautics Program, Hypersonics Project, Experimental Capabilities and Propulsion Disciplines.

References

1. C. V. Shank, "Physics of Dye Lasers", Reviews of Modern Physics, **47**, 649-657 (1975).
2. W. T. Silfvast, *Laser Fundementals 2nd ed.*,Cambridge University Press, 2004.
3. J. P. Webb, "Tunable Organic Dye Lasers", Analytical Chemistry, **44**, 30-46 (1972).

4. A. C. Eckbreth, *Laser Diagnostics for Combustion Temperature and Species* (Gordon & Breach, Amsterdam, Nederland, 1996.

5. W. D. Brobst and J. E. Allen, Jr. “Intracavity Absorption with a continuous wave dye laser: quantification for a narrowband absorber”, Applied Optics, **26**, 3663-3670 (1987).

6. R. C. Spiker, Jr. and J. S. Shirk, “Quantitative Dye Laser Amplified Absorption Spectrometry”, Analytical Chemistry, **46**, 572-574(1974).

7. U. Platt, J. Meinen, D. Pohler, and T. Leisner, “Broadband Cavity Enhanced Differential Optical Absorption Spectroscopy (CE-DOAS) – applicability and corrections” Atmos. Meas. Tech. **2**, 713-723 (2009).

8. S. A. Tedder, J. L. Wheeler, A. D. Cutler, and P. M. Danehy, "Width Increased Dual-pump Enhanced CARS", Applied Optics, **49**, 1305-1313 (2010).

9. T. G. Pavlopoulos, “Scaling of dye lasers with improved laser dyes”, Progress in Quantum Electronics, **26**, 193-224 (2002).

10. R. R. Antcliff and O. Jarrett, Jr. "Multispecies coherent anti-Stokes Raman scattering insturment for turbulent combustion", Rev. Sci. Instrum., **58**, 2075-2079 (1987).

11. R. D. Hancock, K. E. Bertagnolli, and R. P. Lucht, "Nitrogen and Hydrogen CARS Temperature Measurements in a Hydrogen/ Air Flame Using a Near-Adiabatic Flat-Flame Burner", Combustion and Flame, **109**, 323-331 (1997).

12. S. R. Yang, J. R. Zhao, C.J. Sung, and G. Yu, "Multiplex CARS measurements in supersonic H2/air combustion", Applied Physics B, **68**, 257-265 (1999).

13. S. O'Byrne, P. M. Danehy, A. D. Cutler, "Dual-Pump CARS Thermometry and Species Concentration Measurements in a Supersonic Combustor", 42nd Aerospace Sciences Meeting and Exhibit, Reno, Nevada, Jan. 5-8, 2004.

14. E. H. Veen and D. Roekaerts, "Thermometry for turbulent flames by coherent anti-Stokes Raman spectroscopy with simultaneous referencing to the modeless excitation profile", Applied Optics, **44**, 6995-7004 (2005).
15. F. Y. Yueh, and E. J. Beiting, "Simultaneous N2, CO, and H2 multiplex CARS measurements in combustion environments using a single dye laser", Applied Optics, **27**, 3233-3243 (1988).
16. F. Beyrau, T. Seeger, A. Malarski, and A. Leipertz, "Determination of temperatures and fuel/air ratios in an ethene-air flame by dual-pump CARS", J. Raman Spectrosc. **34**, 946-951 (2003).
17. K. Frederickson, S. P. Kearney, and T. W. Grasser, "Dual-Pump CARS Probing of Meter-Scale Turbulent Pool Fires", 45th AIAA Aerospace Sciences Meeting and Exhibit, Reno, NV, January, 7-10, 2008.
18. F. Beyrau, A. Datta, T. Seeger, and A. Leipertz, "Dual-pump CARS for the simultaneous detection of N2, O2, and CO in CH4 flames", Journal of Raman Spectroscopy, **33**, 919-924 (2002).
19. J. Hult, "Construction of a modeless laser for applications in CARS spectroscopy", Master Thesis, Lund 1998.
20. S. P. Kearney and M. N. Jackson, "Dual-Pump Coherent Anti-Stokes Raman Scattering Thermometry in Heavily Sooting Flames", AIAA Journal, **45**, 2947-2956 (2007).
21. A. Malarski, F. Beyrau, and A. Leipertz, "Interference effects of C2-radicals in nitrogen vibrational CARS thermometry using a frequency-doubled Nd:YAG laser", Journal of Raman Spectroscopy, **36**, 102-108 (2004).

22. D. V. Flores, "Analysis of Lean Premixed Turbulent Combustion Using Coherent Anti-Stokes Raman Spectroscopy Temperature Measurements", PhD dissertation, Chemical Engineering Department, Brigham Young University, 2003.

23. J. K. Haslam and P. O. Hedman, “The Use of Two Pyromethene Dyes in a Single Stokes Dye Laser to Make CARS Temperature and Multiple Species (CO, CO_2, O_2, and, N_2) Concentration Measurements”, Fall Meeting of the Western States Section of the Combustion Institute, The University of Southern California, WSS/CI 96F-086, October 26-29, 1996.

24. W.P. Partridge, N. M. Laurendeau, C. C. Johnson, and R. N. Seppel, “Performance of Pyrromethene 580 and 597 in a commercial Nd:YAG-pumped dye-laser system”, Opt. Letters, **19,** 1630-1632 (1994).

25. M. D. Rahn, T. A. King, A. A. Gorman, and I. Hamblett, “Photostability enhancement of Pyrromethene 567 and Perylene Orange in oxygen-free liquid and solid dye lasers”, Applied Optics, **36**, 5862-5871 (1997).

26. A. J. S. McGonigle, A. J. Andrews, G. P. Hogan, D. W. Coutts and, C.E. Webb, “A compact frequency-doubled 10-kHz PRF copper-vapour-laser-pumped dye laser”, Appl. Phys. B, **76**, 307-311 (2003).

27. S. Sinha, A. K. Ray, S. Kundu, Sasikumar, T. B. Pal, S. K. S. Nair, and K. Dasgupta, “Spectral characteristics of a binary dye-mixture laser”, Applied Optics, **41**, 7006-7011 (2002).

28. R. Khare and S. R. Daulatabad, “A non-mixing technique for enhancement of the tuning range of Rhodamine 6G using Rhodamine B”, Optics and Laser Technology, **36**, 27-30 (2004).

29. F. Lopez Arbeloa, J. Banuelos Prieto, V. Martinez Martinez, T. Arbeloa Lopez, and I. Lopez Arbeloa, "Intramolecular Charge Transfer in Pyrromethene Laser Dyes: Photophysical Behaviour of PM 650", ChemPhysChem, **5**, 1762-1771 (2004).
30. P. Juramy, P. Flamant, and Y. H. Meyer, "Spectral Properties of Pulsed Dye Lasers", IEE Journal of Quantum Electronics, **13**, 855-865 (1977).
31. P. Burlamachhi, R. Pratesi, and U. Vanni, "Tunable superradiant emission from a planar dye laser", Applied Optics, **15**, 2684-2689 (1976).
32. G. I. Farmer, B. G. Huth, L. M. Taylor, and M. R. Kagan, "Concentration and Dye Length Dependence of Organic Dye Laser Spectra", **8**, 363-366 (1969).
33. F. P. Schafer, *Dye Lasers Second Revised Edition*, Springer-Verlag, 1977.
34. A. Costela, I. Garcia-Moreno, C. Gomez, F. Amat-Guerri, M. Liras, and R. Sastre, "Efficient and highly photostable solid-state dye lasers based on modified dipyrromethene.BF2 complexes incorporated into solid matrices of poly(methl methacrylate)", App. Phys. B., **76**, 365-369 (2003).
35. S. Mula, A. K. Ray, M. Banerjee, T. Chaudhuri, K. Dasgupta, and S. Chattopadhyay, "Design and Development of a New Pyrromethene Dye with Improved Photostability and Lasing Efficiency: Theoretical Rationalization of Photophysical and Photochemical Properties", J. Org. Chem., **73**, 2146-2154 (2008).
36. T. Lopez Arbeloa, F. Lopez Arbeloa, I. Lopez Arbeloa, I. Garcia-Moreno, A. Costela, R. Sastre, and F. Amat-Guerri, "Correlations between photophysics and lasing properties of dipyrromethene-BF_2 dyes in solution" Chemical Physics Letters, 315-321 (1999).

37. M. F. Koldunov, Y. V. Kravchenko, A. A. Manenkov, and I. L. Pokotilo, "Relation between spectral and lasing properties for dyes of different classes", Quantum Electronics, **34**, 115-119 (2004).

38. L. Liu, N. N. Barashkov, C. P. Palsule, S. Gangopadhyay, and W. L. Borst, "Intermolecular energy transfer in binary systems of dye polymers", Journal of Applied Physics, **88**, 4860-4870 (2000).

39. M. Alvarez, F. Amat-Guerri, A. Costela, I. Garcia-Moreno, M. Liras, and R. Sastre, "Laser emission from mixtures of dipyrromethene dyes in liquid solution and in solid polymeric matrices", Optics Communications, **267**, 469-579 (2006).

40. B. B. Raju and T. S. Varadarajan, "Energy transfer dye laser characteristics of a dye mixture using a new couramin dye as an acceptor", Journal of Luminescence, **55**, 49-54 (1993).

41. Y. Kusumoto, H. Sato, K. Maeno, and S. Yahiro, "Energy Transfer Dye Laser: Confirmation of Energy Transfer by Reabsorption effect", Chemical Physics Letters, **53**, 388-390 (1978).

42. A. K. Ray, S. Kundu, S. Sasikumar, C. S. Rao, S. Mula, S. Sinha, and K. Dasgupta, "Comparative laser performances of Pyrromethene 567 and Rhodamine 6G dyes in copper vapour laser pumped dye lasers", Applied Physics B, **87**, 483-488 (2007).

43. G. Jones II, S. Kumar, O. Klueva, and D. Pacheco, "Photoinduced Electron Transfer for Pyrromethene Dyes", J. Phys. Chem. A, **107**, 8429-8434 (2003).

44. G. Jones II, O. Klueva, S. Kumar, and D. Pacheco, "Photochemical and Lasing Properties of Pyrromethene Dyes", Solid State Lasers X, SPIE, **4267** (2001).

45. J. Banuelos Preito, T. Arbeloa, M. Liras, V. Martinez Martinez, and F. Lopez Arbeloa, "Concerning the color change of Pyrromethene 650 in electron-donor solvents", J. of Photochem. and Photobio. A: Chemister, **184**, 298-305 (2006).

46. N. Tanaka and W. N. Sisk, "The photodegradation of Pyrromethene 567 and Pyrromethene 597 by Pyrromethene 546", Journal of Photochemistry and Photobiology A: Chemistry, **172**, 109-114 (2005).

47. S. A. Tedder, P. M. Danehy, G. Magnotti, A. D. Cutler, "CARS Temperature Measurments in a Combustion-Heated Supersonic Jet", 47th AIAA Aerospace Sciences Meeting, Orlando, Florida, Jan. 508, 2009.

48. W. N. Sisk and W. Sanders, "The concentration dependence of the normalized photostability of 1,3,5,7,8-pentamethyl-2,6-di-t-butylpyrromethene-difluoroborate complex (PM 597) methanol solutions", Journal of Photochemistry and Photobiology A: Chemistry, **167**, 185-189 (2004).

49. M. Pealat, P. Bouchardy, M. Lefebvre, and J.-P. Taran, "Precision of miliplex CARS temperature measurements", Applied Optics, **24**, 1012-1022 (1985).

List of Figure Captions

Figure 1. (Color online)

Drawing of optical setup of the laser. All distances measured with an accuracy of ±0.5 cm.

Figure 2. (Color online)

Transmission curves for spectrally selective optics.

Figure 3. (Color online)

An example of a doubled-peak spectrum demonstrating the type of measurements made to characterize the spectral profile of the laser.

Figure 4. (Color online)

Trends of the characteristics of the laser versus dye concentration. Plotted against concentration are (a) FWHM, (b) range (greater than 10% above maximum intensity), (c) peak and half maximum locations, and (d) percent efficiency. PM 597 was tested at two different excitation energy fluencies (indicated as high efficiency and low efficiency).

Figure 5. (Color online)

The effect of adding PM 650 to PM 597 in the oscillator dye cell on the spectrum emitted from the oscillator. The goal for WIDECARS is shown as a solid thick line.

Figure 6. (Color online)

Trends of the characteristics of the laser versus dye concentration of PM 650, for relatively constant concentrations of PM 597. Some dye mixtures were tested with different excitation energy fluences. In (a) the closed symbols represent half-maximum ranges of the emission peak from PM 597 and the open symbols represent half-maximum ranges of the emission peak from PM 650.

Figure 7. (Color online)

The half-maximum wavelengths versus concentrations of PM 650 added to a ~50 mg/L solution of PM 597 in ethanol at different angles of incidence of the spectral selective optic, TFP. Fitted curves are added to show the general trends of the half-maximum. The shaded regions are the wavelengths of the spectra that have energy higher than the half-maximum. Wavelengths of the WIDECARS half-maximum goals are shown as the thickest lines.

Figure 8. (Color online)

Efficiency of oscillator versus TFP angle of incidence at a range of PM 650 concentrations added to a ~50 mg/L solution of PM 597 in ethanol is shown in (a). FWHM of oscillator versus TFP angle of incidence at a range of PM 650 concentrations added to a ~50 mg/L solution of PM 597 in ethanol is shown in (b).

Figure 9. (Color online)

Wavelengths of amplifier range, half-maximum, and peaks versus angle of incidence of optics placed in the oscillator cavity. The dye concentrations for the oscillator are 91.92 mg/L PM 597 and 10.58 mg/L PM 650. The dye concentrations for the amplifier are 21.7 mg/L R 610 and 8.4 mg/L R640.

Figure 10. (Color online)

Oscillator laser characteristics versus pumping fluence.

Figure 11. (Color online)

Wavelengths of peak, half-maxima, and range from the amplifier for a range of concentrations of Rhodamine dyes in methanol. Shown in (a) are pure R640 solutions in methanol, while shown in (b) are mixtures of R610 and R640 in methanol.

Figure 12. (Color online)

Percent standard deviation of a series of single-shot WIDECARS (Pyrromethene (PM) dye mixture in oscillator and Rhodamine dye mixture in amplifier) laser spectra and Rhodamine dye laser spectra. Relative standard deviation represents the spectral noise or shot-to-shot stability of the laser. Average spectral profiles of the dye laser are shown on a secondary axis.

Figure 1

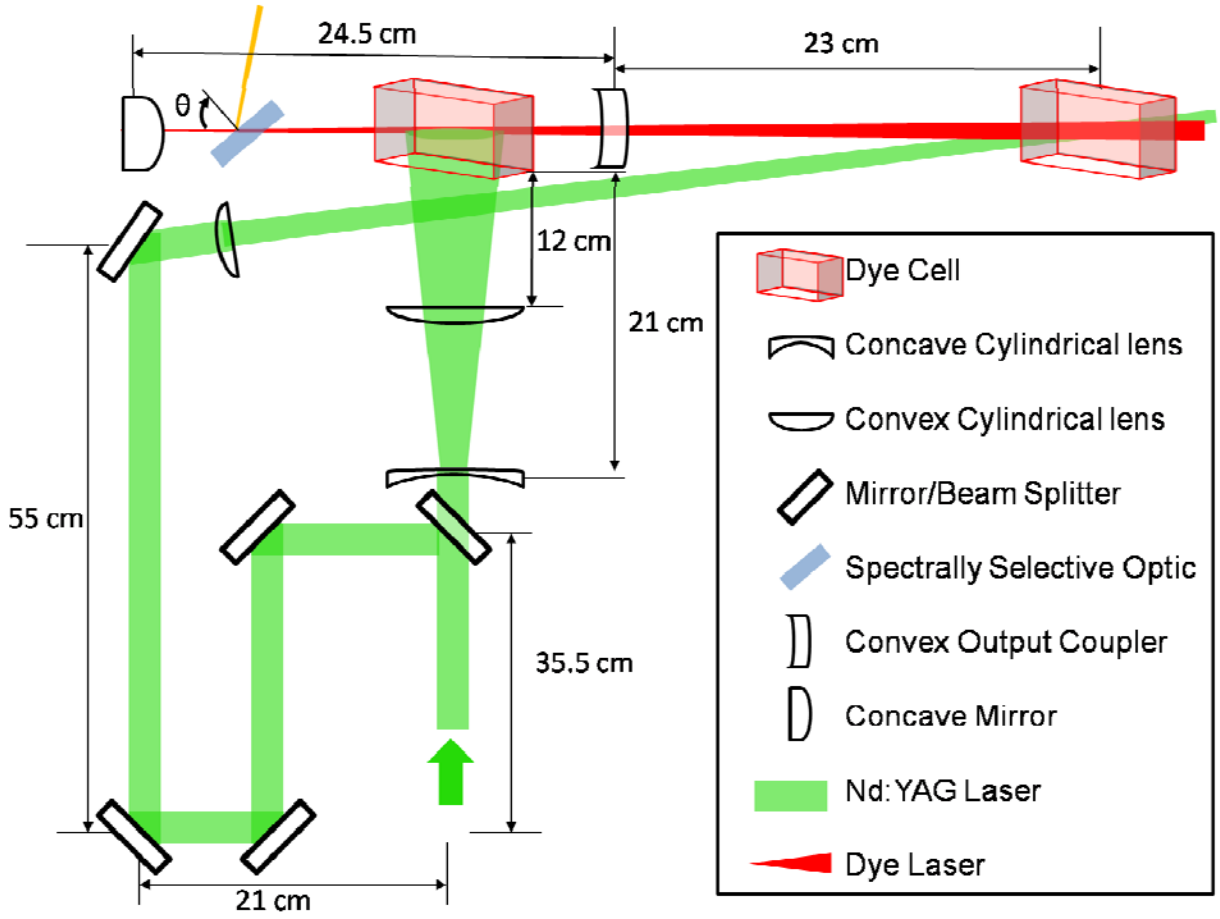
24.5 cm
23 cm
θ
12 cm
21 cm
55 cm
35.5 cm
21 cm
Dye Cell
Concave Cylindrical lens
Convex Cylindrical lens
Mirror/Beam Splitter
Spectrally Selective Optic
Convex Output Coupler
Concave Mirror
Nd:YAG Laser
Dye Laser

Figure 2

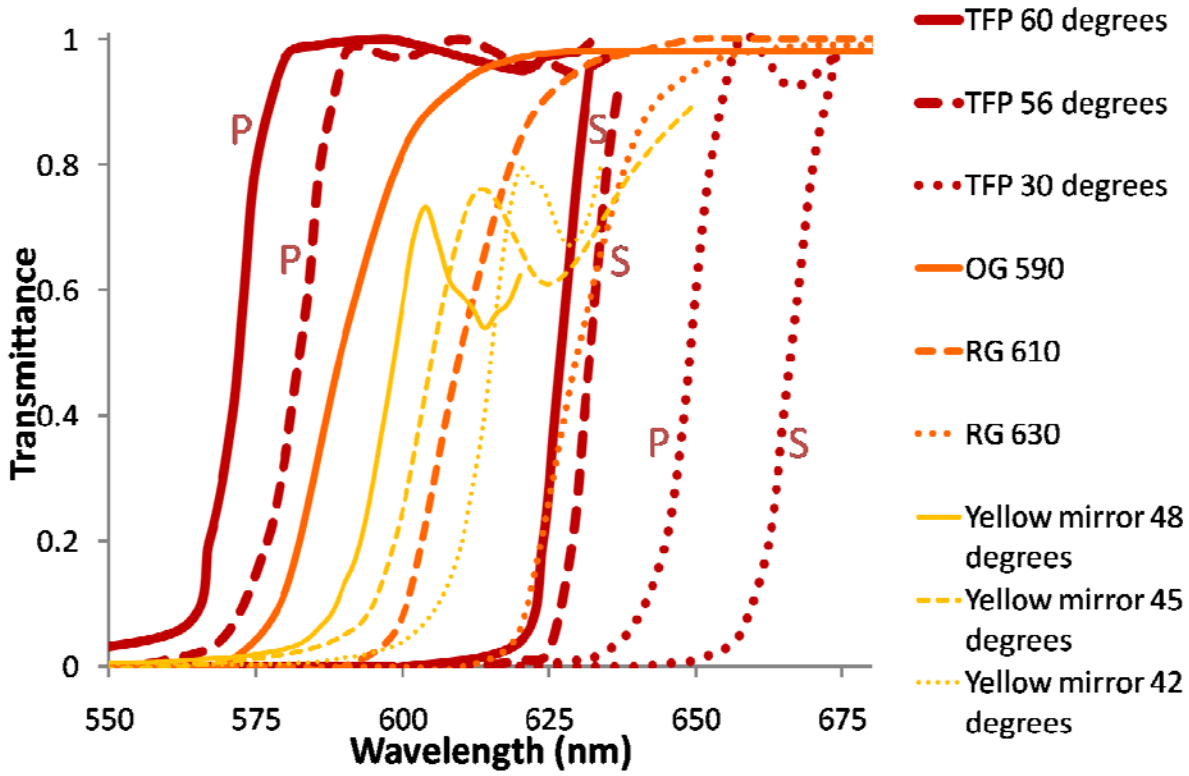
Transmittance
1
0.8
0.6
0.4
0.2
0
550
575
600
625
650
675
Wavelength (nm)
P
P
S
S
P
S
TFP 60 degrees
TFP 56 degrees
TFP 30 degrees
OG 590
RG 610
RG 630
Yellow mirror 48 degrees
Yellow mirror 45 degrees
Yellow mirror 42 degrees

Figure 3

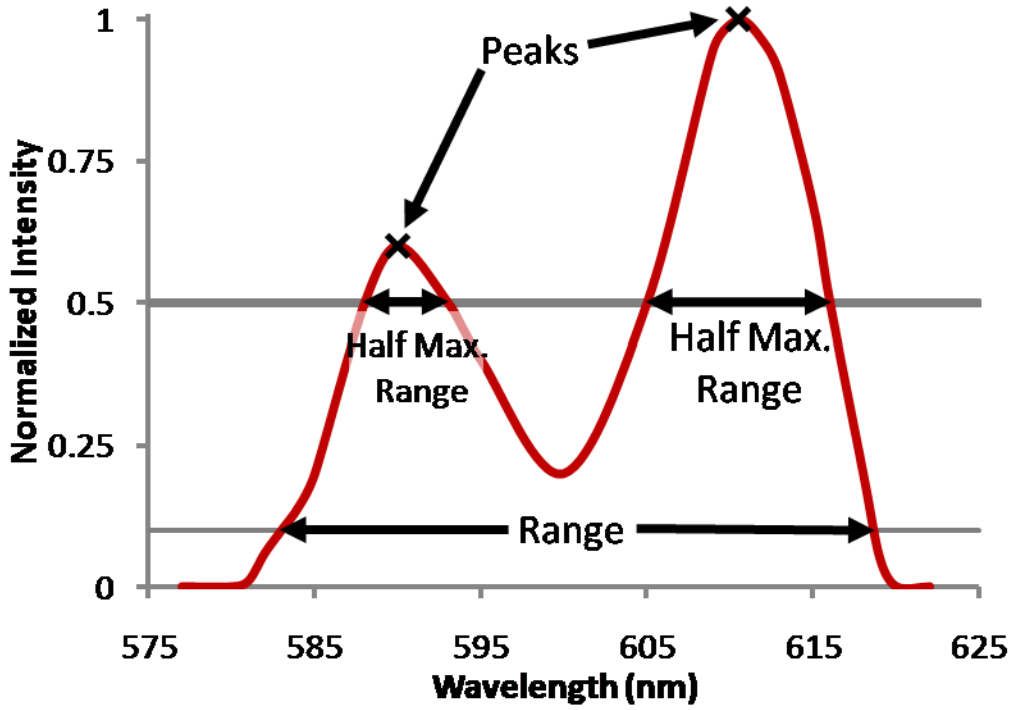
1
0.75
0.5
0.25
0
Normalized Intensity
Peaks
Half Max.
Range
Half Max.
Range
Range
575
585
595
605
615
625
Wavelength (nm)

Figure 4

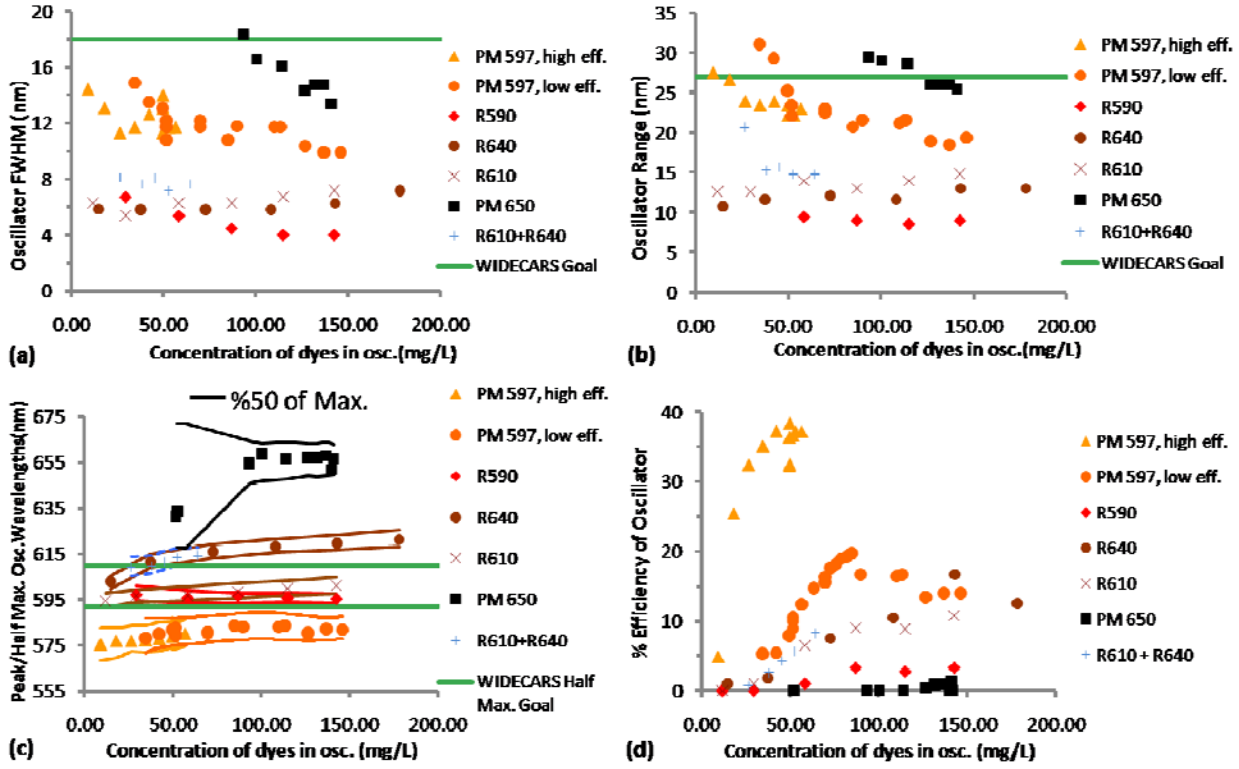
Oscillator FWHM (nm)
Concentration of dyes in osc.(mg/L)
(a)
PM 597, high eff.
PM 597, low eff.
R590
R640
R610
PM 650
R610+R640
WIDECARS Goal
Oscillator Range (nm)
Concentration of dyes in osc.(mg/L)
(b)
%50 of Max.
Peak/Half Max. Osc.Wavelengths(nm)
Concentration of dyes in osc. (mg/L)
(c)
WIDECARS Half Max. Goal
% Efficiency of Oscillator
Concentration of dyes in osc. (mg/L)
(d)
R610 + R640

Figure 5

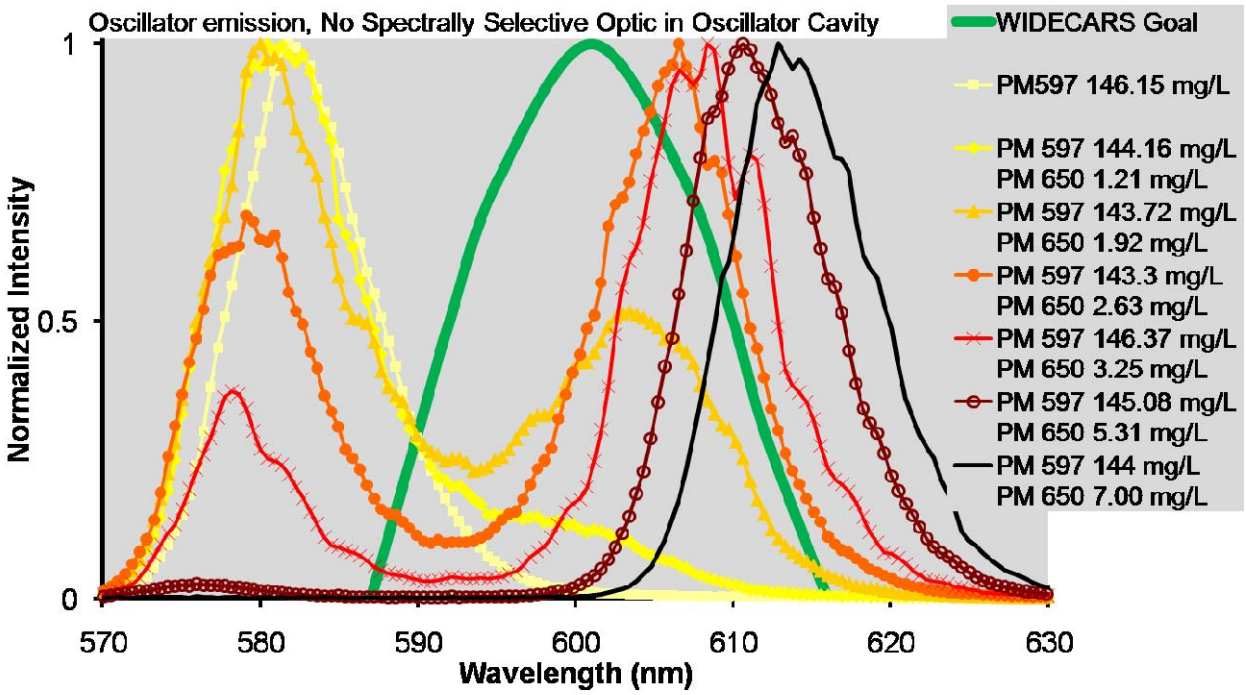
Oscillator emission, No Spectrally Selective Optic in Oscillator Cavity
WIDECARS Goal
PM597 146.15 mg/L
PM 597 144.16 mg/L
PM 650 1.21 mg/L
PM 597 143.72 mg/L
PM 650 1.92 mg/L
PM 597 143.3 mg/L
PM 650 2.63 mg/L
PM 597 146.37 mg/L
PM 650 3.25 mg/L
PM 597 145.08 mg/L
PM 650 5.31 mg/L
PM 597 144 mg/L
PM 650 7.00 mg/L
Normalized Intensity
1
0.5
0
570
580
590
600
610
620
630
Wavelength (nm)

Figure 6

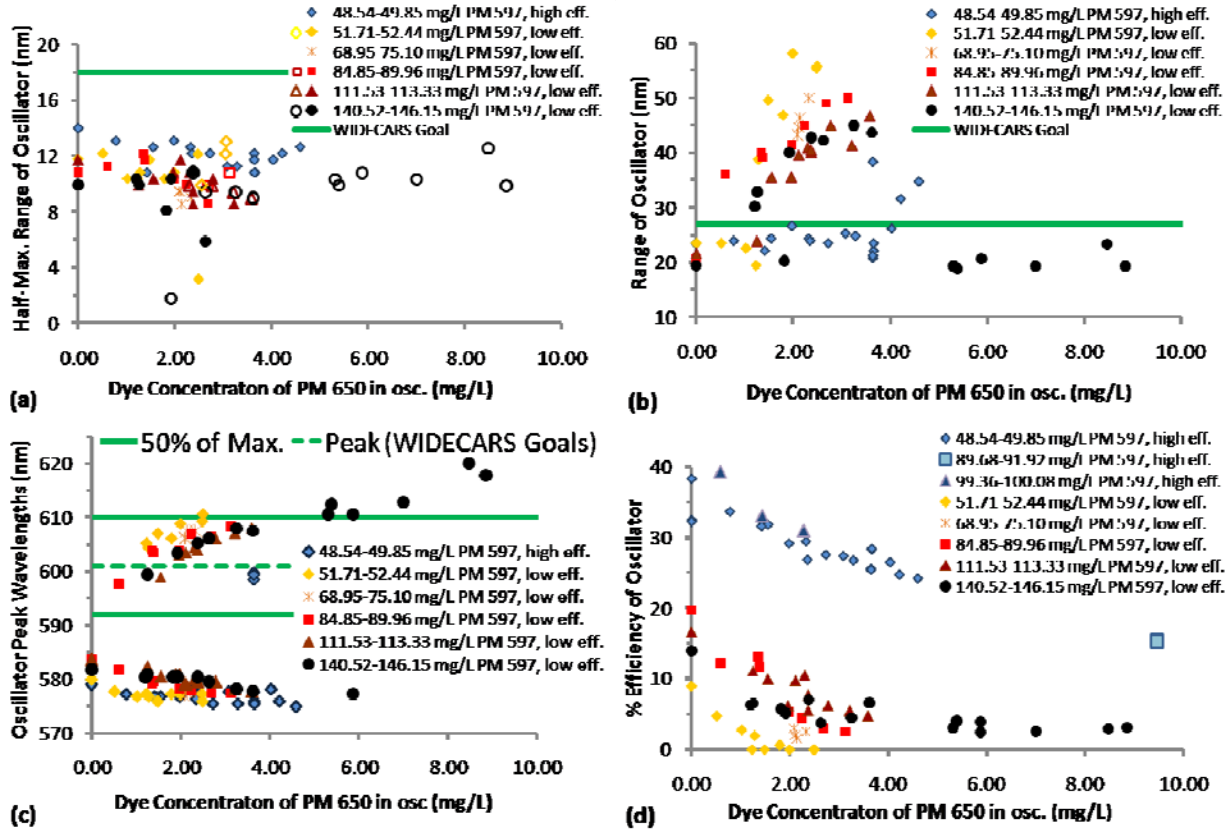
Half-Max. Range of Oscillator (nm)
Dye Concentraton of PM 650 in osc. (mg/L)
(a)
48.54-49.85 mg/L PM 597, high eff.
51.71-52.44 mg/L PM 597, low eff.
68.95 75.10 mg/L PM 597, low eff.
84.85-89.96 mg/L PM 597, low eff.
111.53 113.33 mg/L PM 597, low eff.
140.52-146.15 mg/L PM 597, low eff.
WIDECARS Goal
Range of Oscillator (nm)
Dye Concentraton of PM 650 in osc. (mg/L)
(b)
50% of Max.
Peak (WIDECARS Goals)
Oscillator Peak Wavelengths (nm)
Dye Concentraton of PM 650 in osc (mg/L)
(c)
89.68-91.97 mg/L PM 597, high eff.
99.36-100.08 mg/L PM 597, high eff.
% Efficiency of Oscillator
Dye Concentraton of PM 650 in osc. (mg/L)
(d)

Figure 7

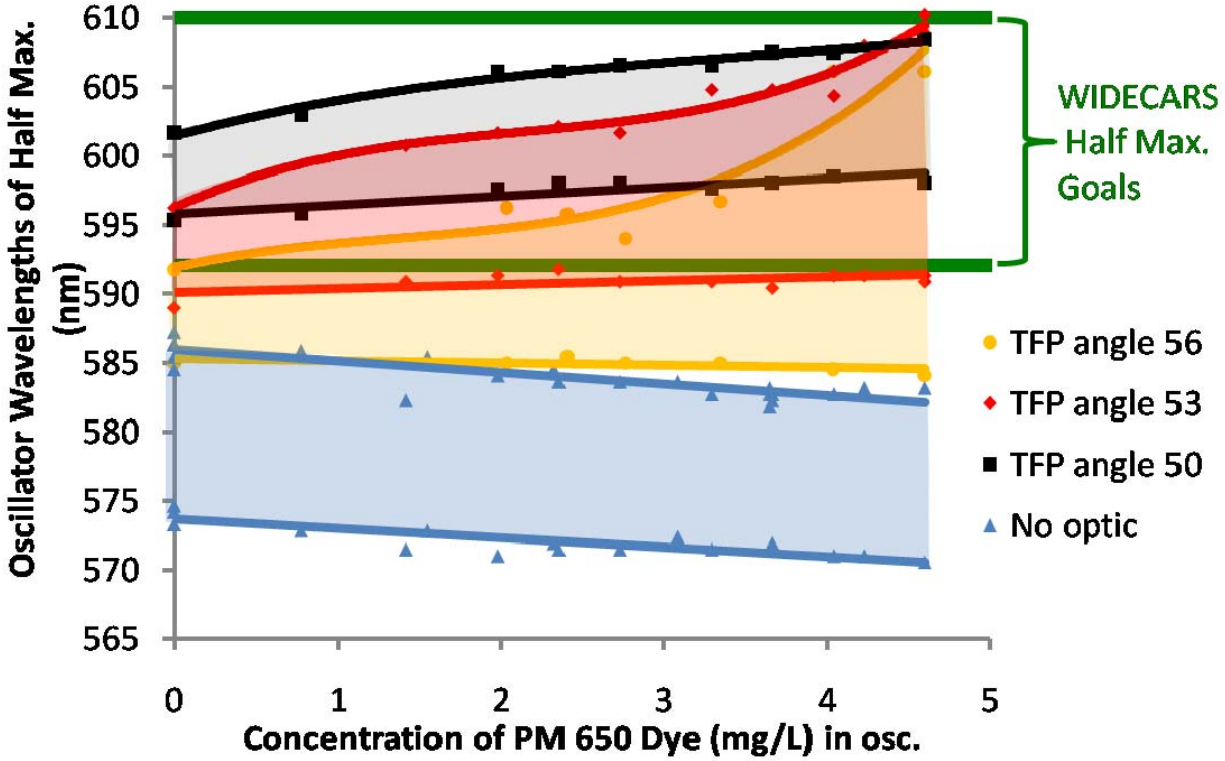
Oscillator Wavelengths of Half Max. (nm)
610
605
600
595
590
585
580
575
570
565
0
1
2
3
4
5
Concentration of PM 650 Dye (mg/L) in osc.
WIDECARS Half Max. Goals
TFP angle 56
TFP angle 53
TFP angle 50
No optic

Figure 8

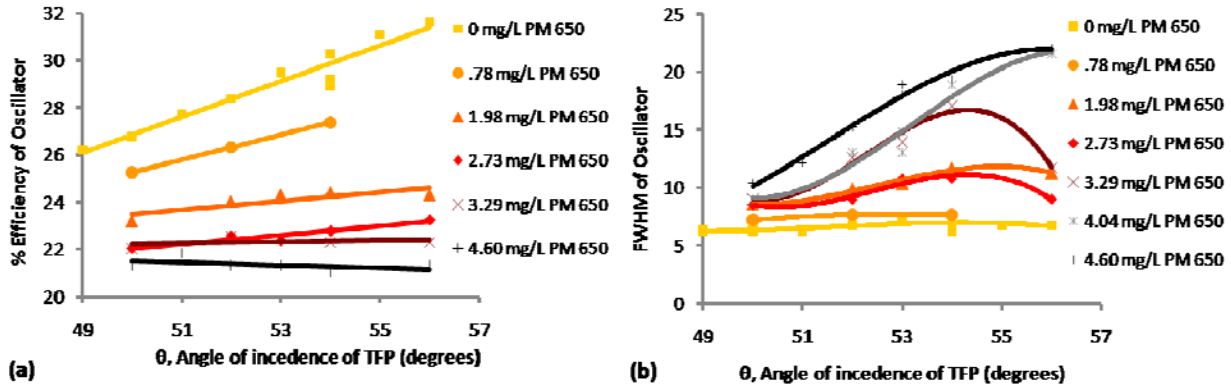
% Efficiency of Oscillator
32
30
28
26
24
22
20
49
51
53
55
57
θ, Angle of incedence of TFP (degrees)
(a)
0 mg/L PM 650
.78 mg/L PM 650
1.98 mg/L PM 650
2.73 mg/L PM 650
3.29 mg/L PM 650
4.60 mg/L PM 650
FWHM of Oscillator
25
20
15
10
5
0
49
51
53
55
57
θ, Angle of incedence of TFP (degrees)
(b)
0 mg/L PM 650
.78 mg/L PM 650
1.98 mg/L PM 650
2.73 mg/L PM 650
3.29 mg/L PM 650
4.04 mg/L PM 650
4.60 mg/L PM 650

Figure 9

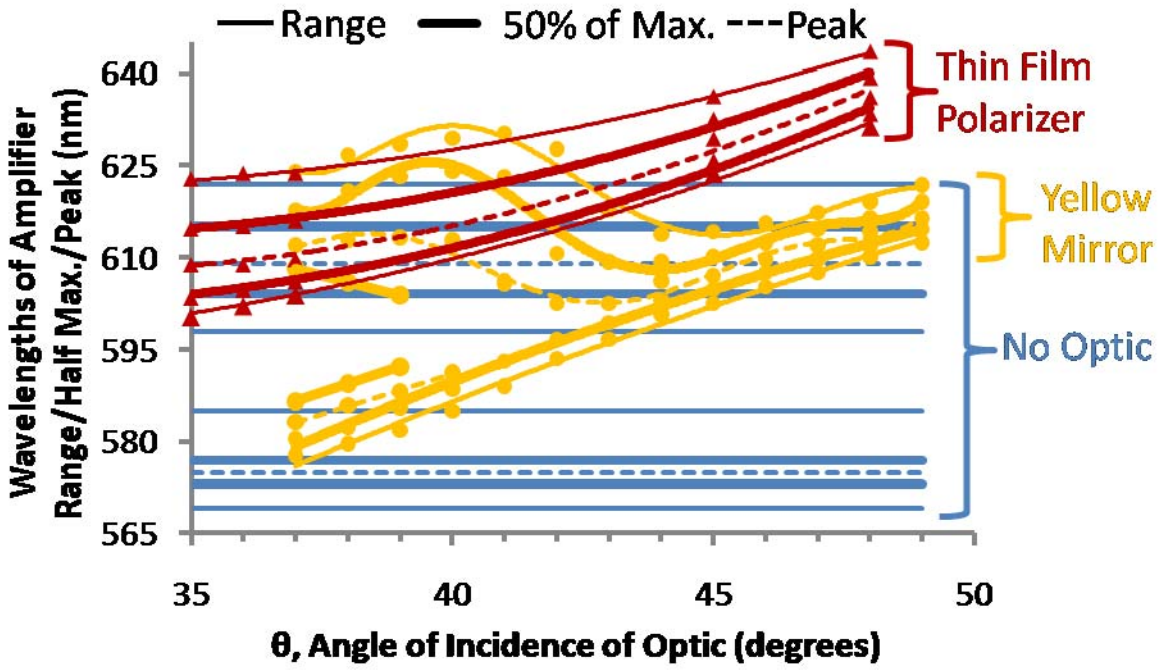
Range
50% of Max.
Peak
Thin Film
Polarizer
Yellow
Mirror
No Optic
Wavelengths of Amplifier
Range/Half Max./Peak (nm)
640
625
610
595
580
565
35
40
45
50
θ, Angle of Incidence of Optic (degrees)

Figure 10

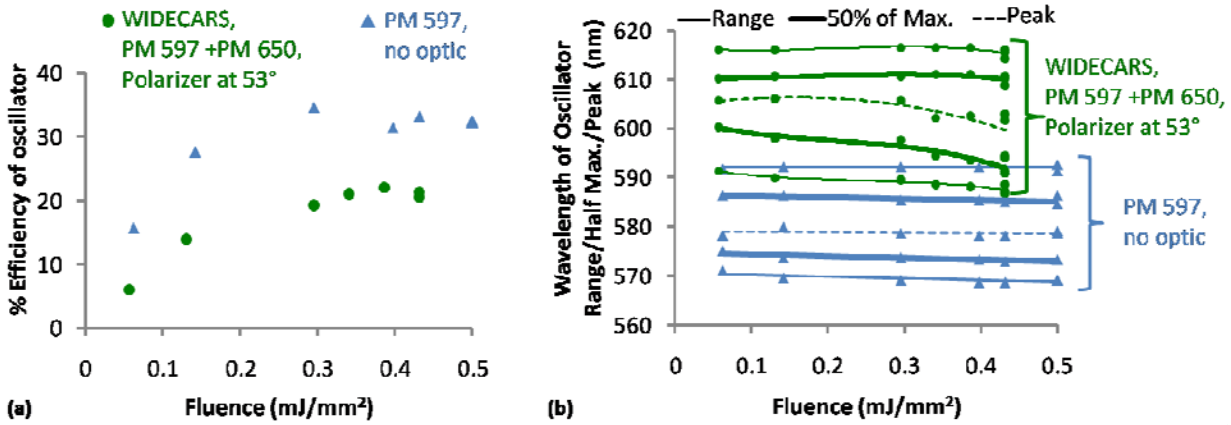
WIDECARS, PM 597 +PM 650, Polarizer at 53°
PM 597, no optic
% Efficiency of oscillator
Fluence (mJ/mm²)
(a)
Range
50% of Max.
Peak
Wavelength of Oscillator Range/Half Max./Peak (nm)
WIDECARS, PM 597 +PM 650, Polarizer at 53°
PM 597, no optic
Fluence (mJ/mm²)
(b)

Figure 11

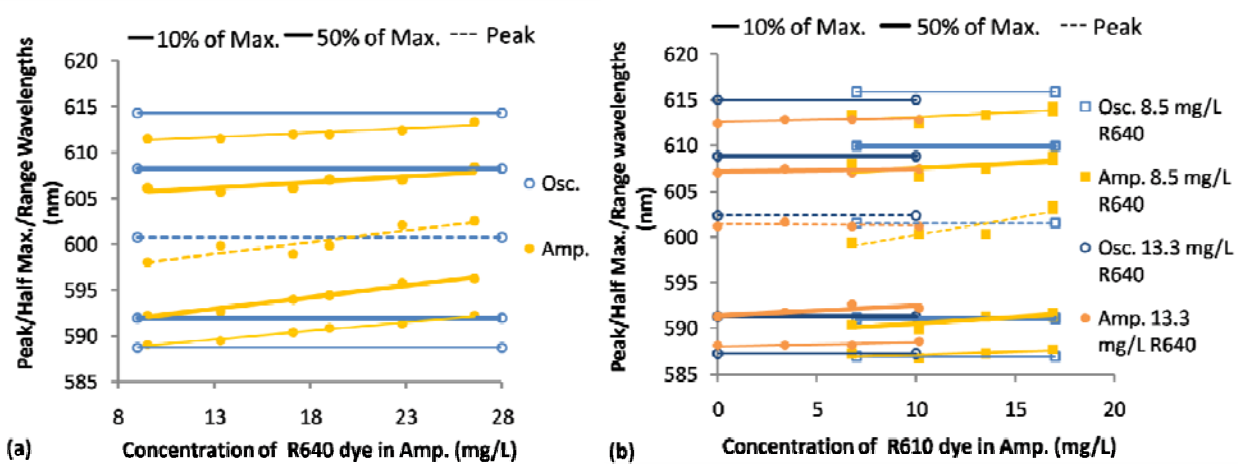
10% of Max.
50% of Max.
Peak
Peak/Half Max./Range Wavelengths (nm)
620
615
610
605
600
595
590
585
8
13
18
23
28
Osc.
Amp.
(a)
Concentration of R640 dye in Amp. (mg/L)
10% of Max.
50% of Max.
Peak
Peak/Half Max./Range wavelengths (nm)
0
5
10
15
20
Osc. 8.5 mg/L R640
Amp. 8.5 mg/L R640
Osc. 13.3 mg/L R640
Amp. 13.3 mg/L R640
(b)
Concentration of R610 dye in Amp. (mg/L)

Figure 12

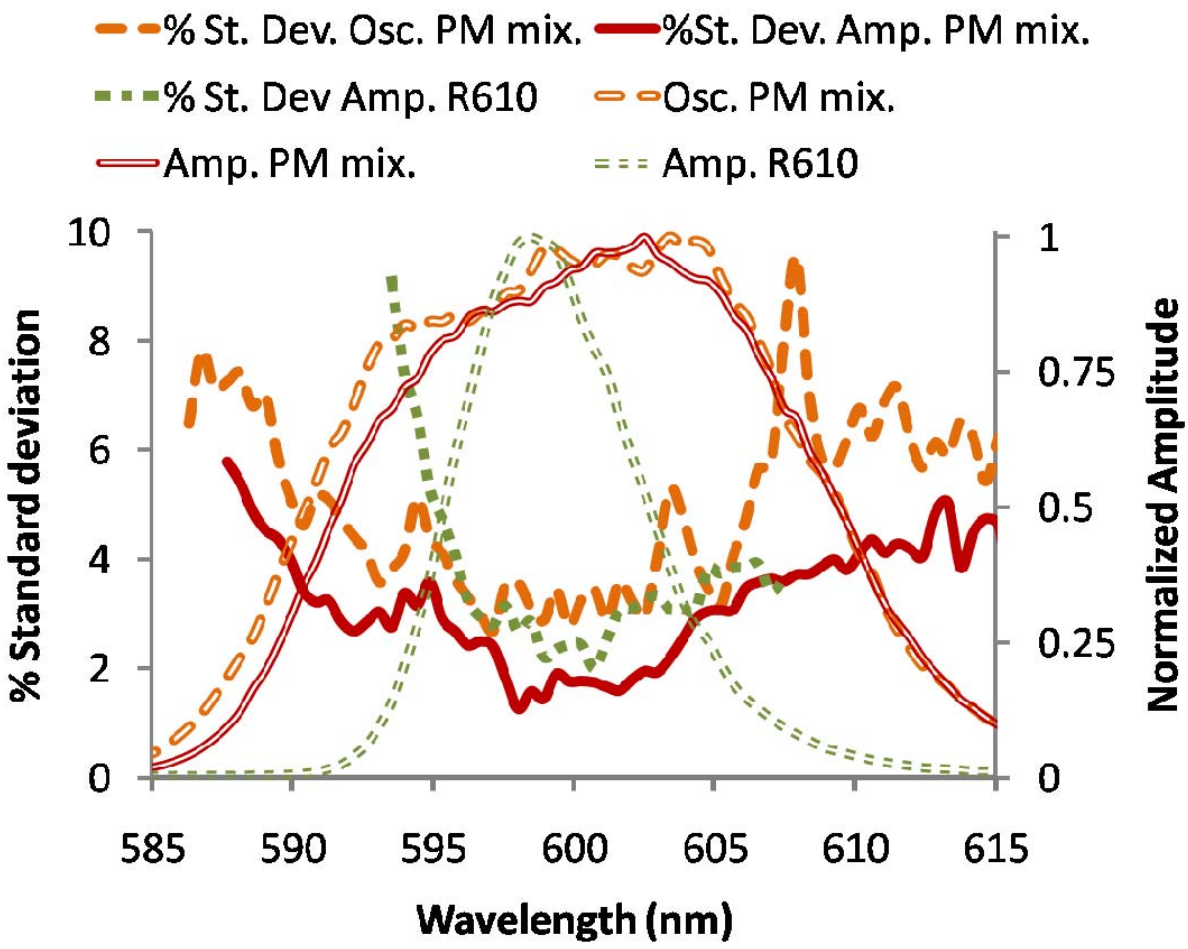
% St. Dev. Osc. PM mix.
%St. Dev. Amp. PM mix.
% St. Dev Amp. R610
Osc. PM mix.
Amp. PM mix.
Amp. R610
% Standard deviation
Normalized Amplitude
Wavelength (nm)
0
2
4
6
8
10
0
0.25
0.5
0.75
1
585
590
595
600
605
610
615